Proceedings of 14th IOE Graduate Conference
Peer Reviewed
Year: 2023 Month: December Volume: 14
ISSN: 2350-8914 (Online), 2350-8906 (Print)

Effect of lateral load on in-plane strength of circular Concrete Filled Steel Tubes (CFST) parabolic arches

Anurag Joshi [a], Bharat Mandal [b], Gokarna Motra [c]

[a, b, c] *Department of Civil Engineering, Pulchowk campus, IOE, Tribhuvan University, Nepal*
[a] 078msste004.anurag@pcampus.edu.np, [b] bharat@ioe.edu.np, [c] gmotra@ioe.edu.np

Abstract
The present study is the examination of the behavior and in-plane strength of Concrete Filled Steel Tube (CFST) arches when acted upon by out of plane loads. When arches are acted upon by spatial loads, they have to resist a combination of axial, bending, shear and torsion all at the same time due to their curved geometry. To resist such combined loading, the steel and concrete interact in a complex manner. The steel provides passive confinement to concrete core enhancing its compressive strength whereas the concrete core prevents premature local buckling of steel tube. A user subroutine was written for ABAQUS FE software in FORTRAN to numerically model such behavior of concrete and steel. Validation of model against experimental results from available literature suggested good agreement. The validated model was used for numerical simulation of twin parabolic arches with suitable spacing, lateral bracings and fixed ends. The results suggest strong sensitivity of in-plane load carrying capacity of arches when acted upon by lateral loads. The in-plane load carrying capacity was decreased by as much as 50% when lateral loads were mere 2.5% of the in-plane loads. This fact suggests the dominating role of out-of-plane forces in the design of CFST Arch bridges.

Keywords
Concrete Filled Steel Tube (CFST), In-plane strength, User-Material (UMAT), Combined Loading, Finite Element (FE)

1. Introduction

1.1 Background

A concrete filled steel tube (CFST) is a structural member consisting of a thin-walled outer steel tube and a concrete core made up of by pouring fresh concrete inside the steel tube. Such structural members have gained wide popularity as compression members of high-rise buildings, piers of bridges as well as the arch rib of CFST arch bridges. The popularity emerges out of the fact that in CFST members the core concrete provides restraint against premature local buckling of steel tube and outer steel jacket provides confining effect to the concrete core which results in superior strength and ductility of CFST members. The seismic performance is also enhanced due to increased ductility. Furthermore, the steel tube itself acts as a formwork for fresh concrete thereby reducing the cost of formwork to bare minimum.

The ultimate structural strength exhibited by a CFST member has been the topic of research for many scholars. In early days, superposition method of strength calculation was popular, which simply was the sum of concrete strength and steel strength modified by some factors [1].

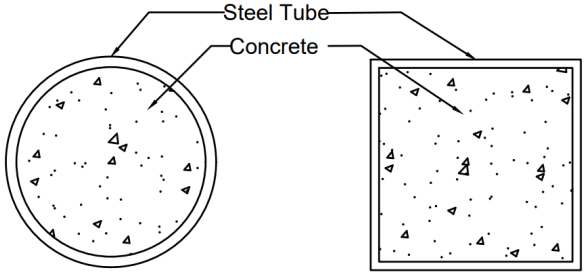

Figure 1: The Cross Section of a Circular and Square CFST Member

To distinguish from the superposition methods of strength calculation as stated above, a “Unified Theory” approach assumes the CFST to be integrated “composite material” and calculations are based on the bulk properties of this “composite material”. This theory predicts the strength of not only a single type of load but of a complex loading state [1, 2].

At present, different methods of finite element modelling of confined concrete have been established. Some involve regression analysis of stress-strain relations from experimental outcomes which are dependent on material and geometrical parameters. These obtained stress-strain relations are then used to calculate stress-strain curves which are inputted to FE software for numerical simulations [2, 3]. With stress-strain relations, Concrete Damaged Plasticity Model (CDPM) with stiffness degradation was also found to be used [4]. Other studies were found to establish parameters for three dimensional plasticity models for concrete such as pressure sensitive Drucker-Prager or extended Drucker-Prager type plasticity [5].

In a study that was originally meant for Fiber Reinforced Polymer (FRP) confined concrete, the stress-strain relations suggested by [3] showed that it was also valid for confinement by steel tube. The difference was that, in FRP confined concrete, the confinement pressure increased linearly with increasing strains until brittle failure of FRP jacket whereas confinement provided by steel showed elasto-plastic behavior. Hence, by substituting the linear stress-strain relations of FRP with elasto-plastic material model of steel, the confined concrete model could be extended to that of CFST.

For finite element modelling of CFST members requires material models for steel and confined concrete. Concrete models to accurately predict the behavior of passively confined concrete must have yield function that includes not only the second but also the third invariant of deviatoric stress, a hardening softening rule and a potential function that depends upon the confinement pressure [5].

A confined concrete model developed by [6] satisfies the above conditions. This model was implemented in ABAQUS as a user material UMAT. The implementation was achieved by use of elastic predictor plastic corrector closest point projection method as this algorithm computes not only the stresses for strains but also the consistent Jacobian which aids faster convergence [7].

1.2 Research Objectives

The primary objectives of this research would be:

- To implement a numerical model in ABAQUS of CFST arch which is valid for combined loading condition.
- To evaluate the ultimate in-plane load carrying capacity of a circular CFST arch pair.
- To evaluate the dependency of in-plane loads on out-of-plane load carrying capacity of a CFST arch ribs.

2. Finite element modelling

The modelling of CFST arch was carried out in ABAQUS FE Software. ABAQUS was selected for the FE analysis because of its flexibility and robustness in modelling and analyzing composite structures as well as its ability to define user subroutines for defining constitutive models not already present in ABAQUS which would be critical for the problem at hand.

2.1 Material Models

2.1.1 Steel

Since, the analysis adopted is non-linear in nature, a non-linear steel stress-strain model is utilized to capture the behavior of steel. The equations to define these non-linear stress-strain equations are based on Ramberg-Osgood equation. The reason for selection of Ramberg-Osgood relation for stress-strain curve is to generalize the range of stress-strain curves of various strengths of steel that could be used as well as provide basic nonlinearity to the material model. The steel stress-strain curve is defined by the equation of Ramberg-Osgood given in Equation 1:

$$\varepsilon = \frac{\sigma}{E_s} + \varepsilon_y \left(\frac{\sigma}{f_y}\right)^{1/n} \tag{1}$$

Where, ε is the strain at stress σ, E_s is the modulus of elasticity, f_y is the yield stress of steel, ε_y is offset strain taken as 0.002 (0.2%), n = $\frac{\ln(f_u/f_y)}{\ln(\varepsilon_u/\varepsilon_y)}$ is Strain hardening coefficient, ε_u is the ultimate strain, f_u is the Ultimate stress.

This stress-strain relation was implemented in ABAQUS as isotropic elasto-plastic material, with stress-plastic strain data obtained from the equation 1.

2.1.2 Concrete

The concrete core in CFST members exhibit the property of confined concrete because of the confinement provided by outer steel tube during compression while in bending and torsion the effect of confinement is negligible accounting for differing behavior according to the geometry and loading. The challenge to model such behavior was accomplished by writing a user subroutine in ABAQUS FE software that critically handles the above property of concrete core in CFST member. The user subroutine UMAT is based on the multiaxial plastic constitutive relation given by [6] and implemented by using closest point projection method. The implemented UMAT takes 4 parameters as input, modulus of elasticity of concrete, poisson's ratio, compressive strength and tensile strength and computes stress increments for given strain increments within the FE framework. The subroutine UMAT also requires the material Jacobian, which needs to be calculated within the UMAT implementation, and its value passed to ABAQUS solver. The calculation of consistent Jacobian aids faster convergence of incremental solvers used to solve the boundary value problem within the FE software.

2.2 Element type, Mesh and Boundary Conditions

The concrete core was assigned an 8-node solid brick element denoted by C3D8 in ABAQUS and the steel jacket was also assigned an 8-node solid brick element C3D8. The mesh was dominated by hexagonal elements.

A surface-to-surface contact formulation was used as the contact interface between steel and concrete. The contact interface was defined to be coulomb friction model in tangential direction with friction factor of 0.6 whereas contact pressure model in normal direction.

The solver used was static general with direct sparse equation solver. The step increment was kept constant with appropriate values of increment depending upon the loading and geometry such that convergence was achieved.

A sample mesh of circular CFST section is shown in Figure 2 as displayed in ABAQUS viewport.

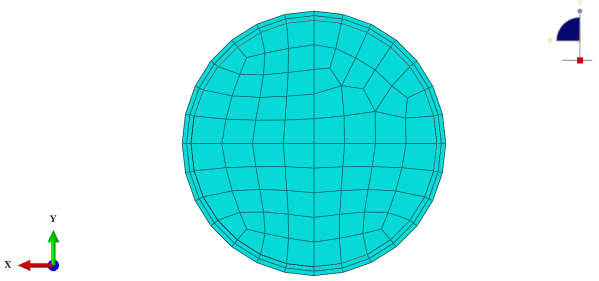

Figure 2: A sample mesh of circular CFST section in ABAQUS Viewport

3. Verification of Model

The developed model was verified against selected literature experimental results for validation of the model. The validation was carried out in two arches, one with in-plane load only [8] and another with both in-plane as well as out-of-plane loading [9].

3.1 Data for verification

Two arches from literature were selected one with in-plane load [8] and another with in-plane and out-of-plane loading [9]. The detail material and geometric parameters are given in Table 1:

Table 1: Details of Material and Geometric parameters for validation

Property	Liu et al. (2017) [8]	Chen et al. (2006) [9]
Span (m)	9	7.5
Rise/Span	1/6	1/5
Rise (m)	1.5	1.5
Diameter (mm)	159	121
Thickness of steel (mm)	4.5	4.5
Yield stress of steel (MPa)	376.2	322
Ultimate stress of steel (MPa)	577.8	523.4
Young's Modulus of steel (GPa)	204	206
Poisson's Ratio of steel	0.29	0.283
Comp. strength of concrete (MPa)	41.6	66.7
Elasticity of Concrete (GPa)	31	35.8
Poisson's Ratio of concrete	0.2	0.2

The arch in [8] is loaded at crown with a vertical concentrated point load whereas the arch in [9] is loaded with vertical concentrated Force at L/6, L/3, L/2, 2L/3, 5L/6 position and horizontal concentrated force at crown that is $1/10^{th}$ of the vertical load.

3.2 Results of Verification

The above two arches were modelled in ABAQUS FE software by mimicking loadings and boundary conditions. The comparison of results from each of the experiments and FE models are summarized below:

3.2.1 In-plane Loaded Arch

Figure 3, 4 & 5 illustrates the displacement-position graph obtained from experiment conducted by [8] and FEM modelling, when maximum crown displacements are 20mm, 45mm and 80mm respectively. Since, in original experiment, the arch has initial imperfections which caused the asymmetric deformation curve whereas in the FEM, being a idealization, has symmetric span-displacement curves. The numerical simulation results agree fairly good with the experimental results.

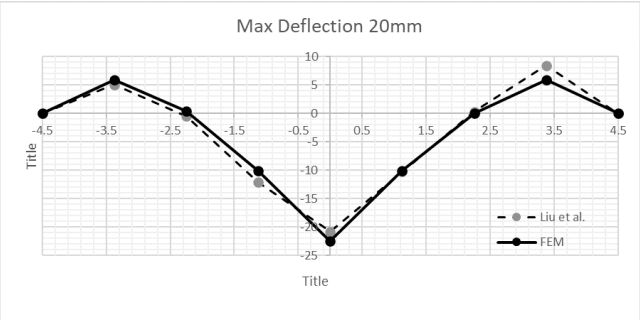

Figure 3: Span-displacement curve at crown displacement of 20mm

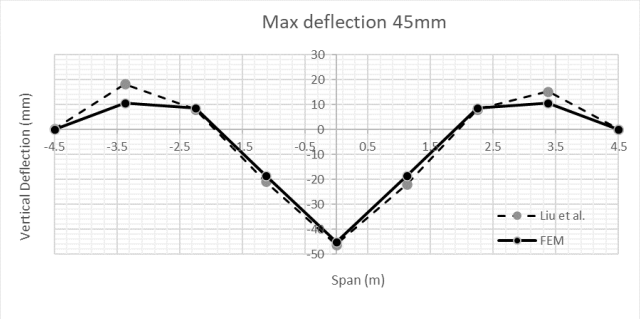

Figure 4: Span-displacement curve at crown displacement of 45mm

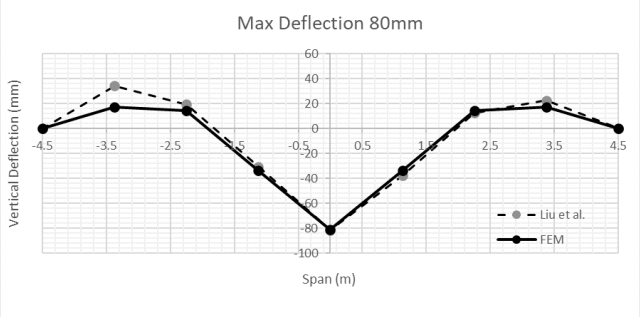

Figure 5: Span-displacement curve at crown displacement of 80mm

3.2.2 In-plane with Out-of-plane Loading

Similarly, for experiment conducted by [9], the load-deformation curves for different positions in the arch are illustrated in Figure 6, Figure 7 & Figure 8 at positions L/2, L/3 and L/6 respectively. The arch was loaded with five equidistant concentrated forces in in-plane direction whereas the out of plane load was applied at the crown position only with intensity of $1/10^{th}$ than that of in-plane load. The comparison of experimental results with FEM results show that they agree quite well. The average error in ultimate load carrying capacity was confined well within 7%. Hence, it was shown that the 3D FE model in ABAQUS performed well in predicting the in-plane as well as out-of-plane behavior of CFST arches.

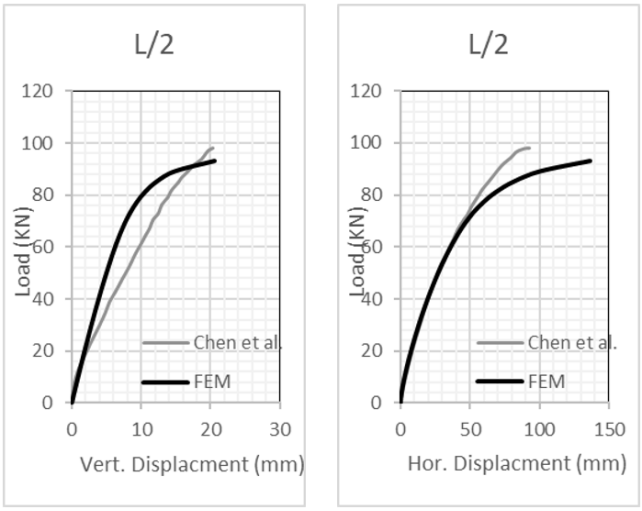

Figure 6: Vertical (Left) and Horizontal(right) Load-displacement curve at position L/2

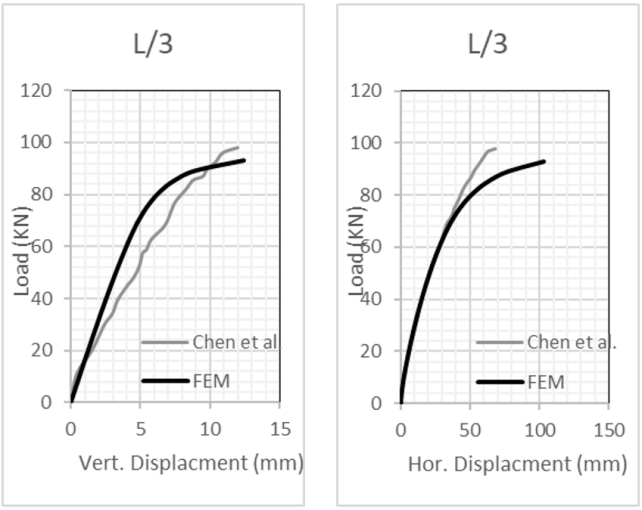

Figure 7: Vertical (Left) and Horizontal(right) Load-displacement curve at position L/3

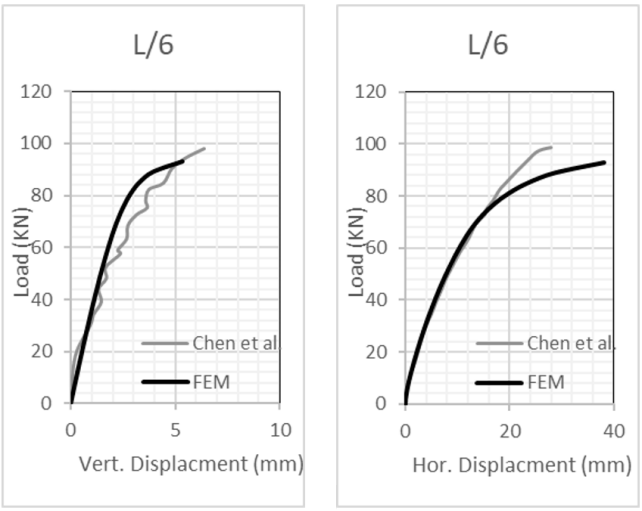

Figure 8: Vertical (Left) and Horizontal(right) Load-displacement curve at position L/6

4. Arches subjected to Lateral loads

The validated model in ABAQUS was used to conduct a series of numerical simulations in twin arches connected by a single vierendeel bracing at the crown and two K-braces placed suitably along the span on both sides. Three arches namely Arch-A, Arch-B and Arch-C which have differing geometry such as different rise-to-span ratio, thickness of steel plate and diameter of arch rib but same material properties, span and spacing of arches were modelled. The complete summary of geometrical and material parameters of the three arches are tabulated in Table 2. The 3D model of the twin arch system acted upon by in-plane and out-of-plane load with fixed boundary condition is illustrated in Figure 9 and details of bracings in Figure 10.

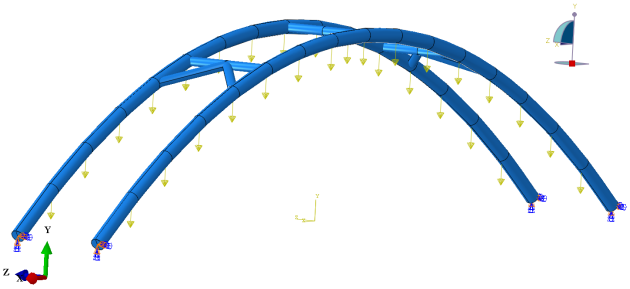

Figure 9: ABAQUS viewport displaying the 3D model of the arch along with boundary conditions

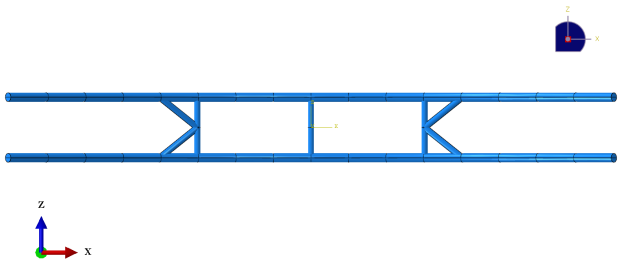

Figure 10: Abaqus Viewport displaying the top view of 3D model of the twin arch with bracings

Table 2: Material and Geometric parameters of arches selected for numerical simulations

Property	Arch A.	Arch B	Arch C
Span (m)	80	80	80
Rise/Span	1/4	1/5	1/6
Rise (m)	20	16	13.33
Diameter (mm)	1500	1200	800
Thickness of steel (mm)	30	20	10
Steel Yield stress (MPa)	325	325	345
Steel Ult. stress (MPa)	520	520	520
Steel Young's Mod. (GPa)	206	206	206
Steel Poisson's Ratio	0.3	0.3	0.3
Conc. comp. Strength (MPa)	32.4	32.4	32.4
Conc. Elasticity (GPa)	34.5	34.5	34.5
Conc. Poisson's Ratio	0.2	0.2	0.2

4.1 Load Displacement characteristics

Each arch were subjected to increasing lateral loads equal to 0%, 2.5%, 5%, 7.5% and 10% of Vertical loads. The complete load-displacement curves with increasing lateral loads of Arch-C are illustrated in Figure 11 through 15.

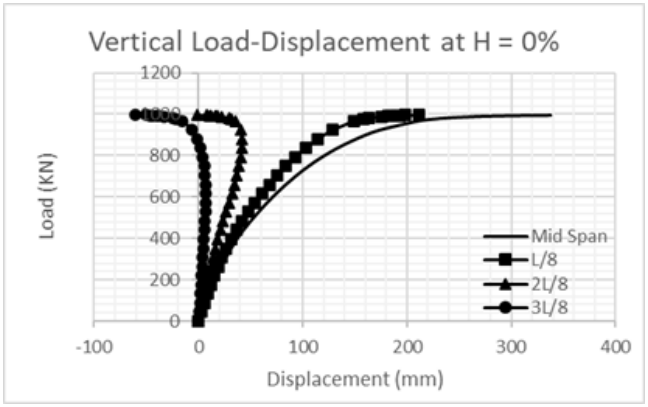

Figure 11: Vertical load-displacement curve of Arch C at 0% Horizontal Load

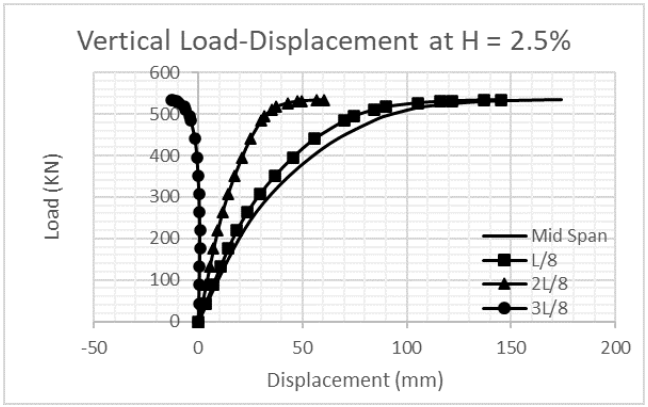

Figure 12: Vertical load-displacement curve of Arch C at 2.5% Horizontal Load

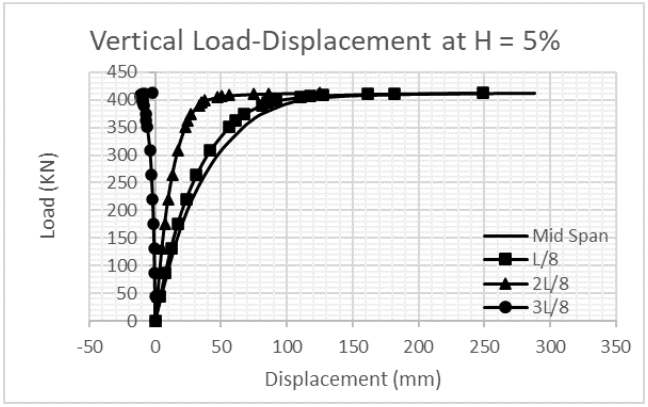

Figure 13: Vertical load-displacement curve of Arch C at 5% Horizontal Load

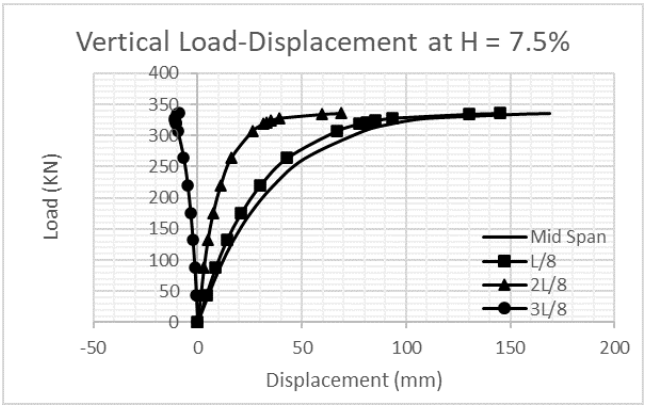

Figure 14: Vertical load-displacement curve of Arch C at 7.5% Horizontal Load

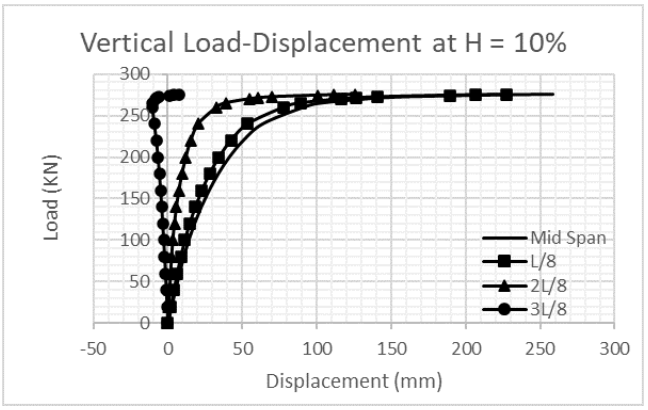

Figure 15: Vertical load-displacement curve of Arch C at 10% Horizontal Load

These curves show that with increase in lateral load, the ultimate in-plane load carrying capacity of the CFST arches progressively deteriorate. The rate of decrease in in-plane load carrying capacity is more during the first few percentages of lateral loads.

4.2 Ultimate Strength of Arches

Figure 16 to 18 illustrates the variation of ultimate strength of CFST arches subjected to increasing lateral loads. The graphs show initial steep decrement of in-plane load carrying capacity which levels off thereafter.

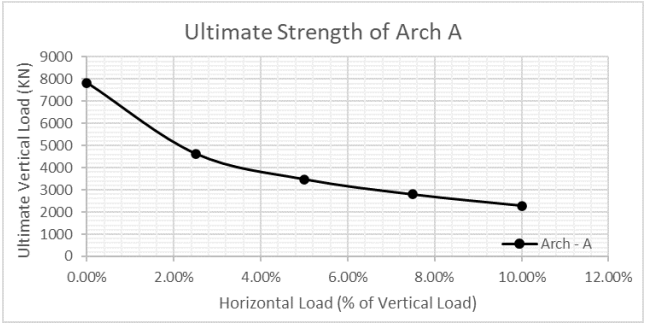

Figure 16: Graph showing decrement of in-plane load carrying capacity with increase in lateral load of Arch A

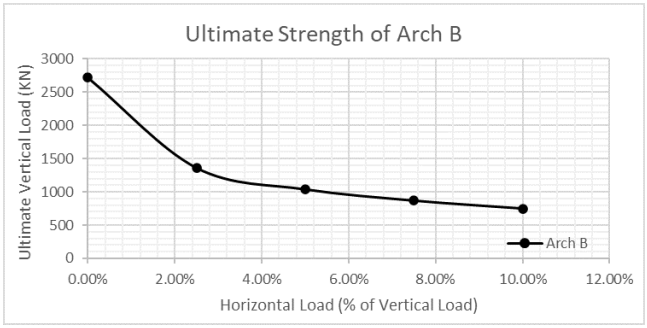

Figure 17: Graph showing decrement of in-plane load carrying capacity with increase in lateral load of Arch B

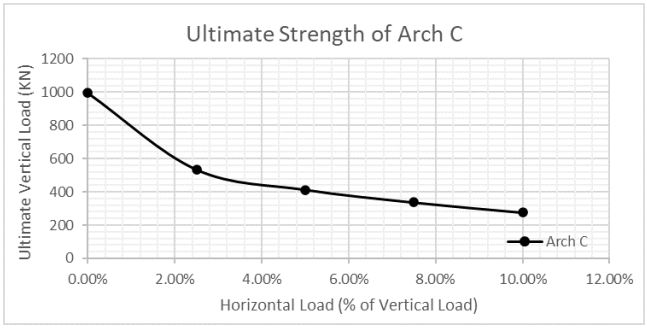

Figure 18: Graph showing decrement of in-plane load carrying capacity with increase in lateral load of Arch C

5. Discussion on Results

Three arches Arch A, B and C were modelled in ABAQUS/CAE and these arches were first loaded in-plane up to their ultimate loads by equal concentrated forces at 5m interval resembling suspenders. After ultimate vertical loads were obtained by applying gradually increasing vertical loads each arch was reloaded by 2.5%, 5%, 7.5% and 10% of vertical loads as horizontal loading. Hence each of the three arches were subjected to purely vertical loads and vertical loads with 2.5%, 5%, 7.5% and 10% horizontal loading.

Figure 16, 17 and 18 for all three arches clearly display the sensitivity of out-of-plane forces in reducing the in-plane strength of the CFST arches. The ultimate in-plane load carrying capacity of the arches decreased by 40.8%, 49.98%, 46.35% for arch A, B and C with increase of horizontal forces from zero to mere 2.5% of vertical loads.

The ultimate vertical load carrying capacity of each of the arches were dependent on the percentage of vertical load applied as horizontal load. With increase in horizontal loading the vertical load carrying capacity decreased remarkably up to 50% of original value within first few percentages. The rate of decrease in strength decreased with increasing horizontal loads which means that the fixed arch pair is extremely sensitive to horizontal loads even when the horizontal loads are very small.

The above discussion supports the fact that lateral load acts as a dominating factor in the design of CFST arch bridges with twin arch parallel ribs.

6. Conclusion

In this paper, 3D FE model of CFST arches were created using ABAQUS/CAE and were validated against the literature for in-plane as well as out-of-plane behavior. The validated model was used to predict the ultimate in-plane load carrying capacity of three arches when acted upon by lateral loads. The results concluded the following:

- The result of validation of model concludes that constitutive model given by [6] can fairly accurately model the confined concrete in CFST members under combined loading conditions.
- The numerical simulation of three arches with varying geometry concludes that the load-deformation behavior is highly dependent on the applied lateral loading.
- The in-plane strength could be reduced by as much as 50% with the application of mere 2.5% of lateral loads.
- This strong dependence of in-plane load carrying capacity on lateral loads suggests that lateral loads are the dictating factor for design of fixed parabolic CFST arch bridges.

Since, the literature suggests that material models of FRP confined concrete could be extended to CFST by using elasto-plastic stress-strain of steel instead of linear stress-strain of FRP, it strongly indicates that the currently developed model would be suitable for describing the behavior of FRP confined concrete, which is suggested for future work.

References

[1] Shan-Tong Zhong and Sumei Zhang. Application and development of concrete-filled steel tubes (cfst) in high rise buildings. *Advances in Structural Engineering*, 2(2):149–159, 1999.

[2] Lin-Hai Han, Guo-Huang Yao, and Zhong Tao. Behaviors of concrete-filled steel tubular members subjected to combined loading. *Thin-Walled Structures*, 45(6):600–619, 2007.

[3] J. G. Teng, Y. L. Huang, L. Lam, and L. P. Ye. Theoretical model for fiber-reinforced polymer-confined concrete. *Journal of Composites for Construction*, 11(2):201–210, 2007.

[4] T. Yu, J.G. Teng, Y.L. Wong, and S.L. Dong. Finite element modeling of confined concrete-ii: Plastic-damage model. *Engineering Structures*, 32(3):680–691, 2010.

[5] T. Yu, J.G. Teng, Y.L. Wong, and S.L. Dong. Finite element modeling of confined concrete-i: Drucker–prager type plasticity model. *Engineering Structures*, 32(3):665–679, 2010.

[6] Peter Grassl, Dimitrios Xenos, Ulrika Nyström, Rasmus Rempling, and Kent Gylltoft. Cdpm2: A damage-plasticity approach to modelling the failure of concrete. *International Journal of Solids and Structures*, 50(24):3805–3816, 2013.

[7] A. Anandarajah. *Computational Methods in Elasticity and Plasticity: Solids and Porous Media*. SpringerLink : Bücher. Springer New York, 2011.

[8] Changyong Liu, Yuyin Wang, Xinrong Wu, and Sumei Zhang. In-plane stability of fixed concrete-filled steel tubular parabolic arches under combined bending and compression. *Journal of Bridge Engineering*, 22, 02 2017.

[9] Bee Chen, J.-G Wei, and J.-Y Lin. Experimental study on concrete filled steel tubular (single tube) arch with one rib under spatial loads. *Gongcheng Lixue/Engineering Mechanics*, 23:99–106, 05 2006.